Real Time Exfoliation Behavior of Clay Layers in Epoxy−Clay Nanocomposites

Doil Kong and Chan Eon Park*

Polymer Research Institute, Department of Chemical Engineering, Electrical & Computer Engineering Division, Pohang University of Science & Technology (POSTECH), Pohang 790-784, Republic of Korea

Received May 17, 2002. Revised Manuscript Received October 30, 2002

Exfoliation behavior of clay layers in epoxy−clay nanocomposites was studied with the electronegativities of aromatic diamine curing agents and curing temperatures. While faster gelation in the extragallery region accelerated by much more reactive aromatic diamine curing agents (1, 3-phenylendiamine (PDA) and 4, 4′-methylenedianiline (MDA)) produced the intercalated structure (<10 nm of *d* spacing), a well-exfoliated nanostructure (>20 nm) was obtained from the slow curing rate of diglycidyl ether of bisphenol A (DGEBA)−4,4′-diaminodiphenyl sulfone (DDS). The exfoliation trend of the clay layer has a unique S-shape pattern with increasing extent of conversion at any curing temperatures. A three-step increase of interlayer distance was found in real time small-angle X-ray diffraction patterns on a polymerizing DGEBA−DDS−C18 clay nanocomposite.

Introduction

During the past decade, polymer nanocomposites with layered silicates (clays) have been intensively investigated and commercialized for their novel physical properties including mechanical properties (modulus, strength, fracture toughness, and surface hardness),[1−3] barrier property,[4−6] flammability resistance,[7] and solvent (or water) uptake,[8,9] compared to the unmodified resin or conventional polymer composite that uses inorganic fillers. It is also interesting to note that these improvements are achieved with less than several volume percent addition of a complete nanoscale dispersion (exfoliated) of 1-nm-thick layered silicate with several hundred nanometers of diameter, while a conventional polymer composite would have to be mixed with more than 30−40 vol % of inorganic fillers such as talc, mica, silica, and carbon black to have equivalent physical properties.[2] Thus, clay as an inorganic nanofiller in a polymer nanocomposite also has advantages in its processing ability, cost, and clarity.

Thermoset polymer−clay nanocomposites, for example, epoxy−clay nanocomposites, have been studied with various curing agents (aliphatic polyamine,[10−16] aromatic diamine,[17−21] anhydride,[17,21−23] and catalytic curing agent[17]), organic surface modifiers[22−24] (aminocarboxilic acid, primary alkyldiamine, and primary alkylmonoamine), and several kinds of clay having different charge densities[12−13,18] (montmorillinite, hectorite, fluorohectorite, vermiculite, and magadiite).

Summarizing the major reports to date, well-dispersed and fully exfoliated epoxy−clay nanocomposites come from intergallery self-polymerization enhanced with a catalytic role of acidic primary alkylammonium surfactant and delaying extragallery matrix gelation.[18]

Then what happens to the clay layer during polymerization in the thermoset−clay nanocomposite system? For polymer melt intercalation (intercalation of "prepolymerized linear macromolecule"), many theoretical and experimental investigations have been carried out

* To whom correspondence should be addressed. E-mail: cep@postech.ac.kr. Tel: +82-54-279-2269. Fax: +82-54-279-8298.

(1) Okada, A.; Kawasumi, M.; Usuki, A.; Kojima, Y.; Kurauchi, T.; Kumigato, O. *Mater. Res. Soc. Symp. Proc.* **1990**, *171*, 45.
(2) Kojima, Y.; Usuki, A.; Kawasumi, M.; Okada, A.; Fukushima, Y.; Kurauchi, T.; Kamigaito, O. *J. Mater. Res.* **1993**, *8*, 1185.
(3) Giannelis, E. P. *JOM* **1992**, *44*, 28.
(4) Yano, K.; Usuki, A.; Okada, A.; Kurauchi, T.; Kamigaito, O. *J. Polym. Sci., A: Polym. Chem.* **1993**, *31*, 2493.
(5) Yano, K.; Usuki, A.; Okada, A. *J. Polym. Sci., A: Polym. Chem.* **1997**, *35*, 2289.
(6) Lan, T.; Kaviratna, P. D.; Pinnavaia, T. J. *Chem. Mater.* **1994**, *6*, 573.
(7) Gilman, J. W.; Kashiwagi, T.; Lichtenhan, J. D. *SAMPE J.* **1997**, *33*, 40. Gilman, J. *Appl. Clay Sci.* **1999**, *15*, 31.
(8) Kojima, Y.; Usuki, A.; Kawasumi, M.; Okada, Y.; Kurauchi, T.; Kamigaito, O. *J. Appl. Polym. Sci.* **1993**, *49*, 1259.
(9) Burnside, S. D.; Giannelis, E. P. *Chem. Mater.* **1995**, *7*, 1597.
(10) Lan, T.; Pinnavaia, T. J. *Chem. Mater.* **1994**, *6*, 2216.
(11) Shi, H.; Lan, T.; Pinnavaia, T. J. *Chem. Mater.* **1996**, *8*, 1584.
(12) Wang, Z.; Lan, T.; Pinnavaia, T. J. *Chem. Mater.* **1996**, *8*, 2200.
(13) Wang, Z.; Lan, T.; Pinnavaia, T. J. *Chem. Mater.* **1998**, *10*, 1820.
(14) Brown, J. M.; Curliss, D.; Vaia, R. A. *Chem. Mater.* **2000**, *12*, 3376.
(15) Kornmann, X.; Lindberg, H.; Berglund, L. A. *Polymer* **2001**, *42*, 1303.
(16) Zerda, A. S.; Lesser, A. J. *J. Polym. Sci., B: Polym. Phys.* **2001**, *39*, 1137.
(17) Messersmith, P. B.; Giannelis, E. P. *Chem. Mater.* **1994**, *6*, 1719.
(18) Lan, T.; Kaviratna, P. D.; Pinnavaia, T. J. *Chem. Mater.* **1995**, *7*, 2144.
(19) Kornmann, X.; Lindberg, H.; Berglund, L. A. *Polymer* **2001**, *42*, 4493.
(20) Chin, I.; Thurn-Albrecht, T.; Kim, H.; Russell, T. P.; Wang, J. *Polymer* **2001**, *42*, 5947.
(21) Lu, J.; Ke, Y.; Qi, Z.; Yi, X. *J. Polym. Sci., B: Polym. Phys.* **2001**, *39*, 115.
(22) Zilg, C.; Mülhaupt, R.; Finter, J. *Macromol. Chem. Phys.* **1999**, *200*, 661.
(23) Zilg, C.; Thomann, R.; Finter, J.; Mülhaupt, R. *Macromol. Mater. Eng.* **2000**, *280/281*, 41.
(24) Wang, M. S.; Pinnavaia, T. J. *Chem. Mater.* **1994**, *6*, 468.

10.1021/cm0205837 CCC: $25.00 © 2003 American Chemical Society
Published on Web 12/17/2002

from thermodynamic and kinetic viewpoints.[25−32] It was relatively easy to approach kinetics or simulation studies about the polymer melt intercalation because of the well-established statistical and thermodynamic background, compared to that about a growing polymer or a three-dimensional cross-linking polymer. Most reports on cross-linking polymer−clay nanocomposites derived through polymerizing the intercalated monomer, so-called "in-situ polymerization method", determined just the optimum manufacturing condition of the exfoliated nanostructure by investigating the initial and the final state of clay layers. There is little information about the exfoliation kinetics of the clay layer in cross-linking polymer−clay nanocomposites during polymerization, although understanding this process became fundamental for ascertaining structure−property relations. Therefore, many things to examine are still stacked in cross-linking polymer−clay nanocomposite fields. For example, by what mechanism is the clay layer exfoliated during the polymerization in the cross-linking polymer−clay nanocomposite? What difference is there in the delamination behavior of the intercalated and the exfoliated nanocomposite? How does the network structure of the cross-linking polymer in the intergallery region compare to that in the extragallery region? Studies addressing these questions may give new insight into growing polymer in the confined layer on a nanometer scale, offering good source data for developing and modifying thermoset−clay nanocomposites for industrial applications.

In this paper, we report not only on the optimum manufacturing conditions of the exfoliated nanostructure but also on the exfoliation kinetics of the clay layer from the initial intercalation of monomer to the final cross-linking step. By monitoring the change in the integrated intensity of the basal reflection of the clay layer, we determined the intercalation condition of the monomer and then investigated the exfoliation behavior on polymerizing with various reactive aromatic amine curing agents at various isothermal curing temperatures. Also discussed are the effects of the reactivity of aromatic amines to epoxy on exfoliation of the clay layer and the relation between the extent of conversion (polymerization) and exfoliation of the clay layer.

Experimental Section

Materials. Na^+−montmorillonite was used as a layered silicate (clay): SWy-2 purchased from the Source Clay Repository at the University of Missouri had 96 mequiv/100 g of the cation exchange capacity (CEC) determined by the total amount of Na^+ ion replaced with ammonium saturated solution. Octadecylamine (C18 amine) was used as an organic modifier of the layered silicates. YD-128 provided by the Kukdo Chemical Co. in Korea was used as an epoxy resin, which is diglycidyl ether of bisphenol A (DGEBA) having an epoxy equivalent weight of 184−190 g/equiv. Aromatic diamines with different electronegativities of the amine groups were used as curing agents: 1,3-phenylenediamine (PDA), 4,4′-methylenedianiline (MDA), and 4,4′-diaminodiphenyl sulfone (DDS). The organic modifier and amine curing agents were purchased from the Aldrich Co. and used without further purification. The chemical structures used are shown in Figure 1.

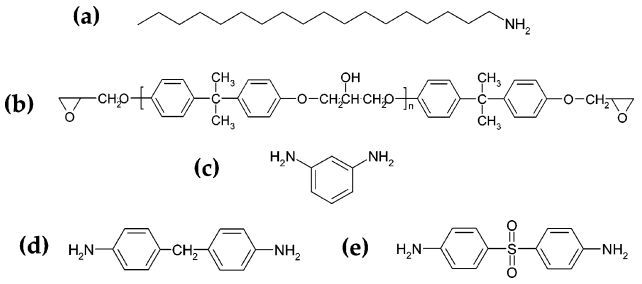

Figure 1. Chemical structure of organic surfactants, epoxy prepolymer, and aromatic diamines: (a) octadecylamine (C18 amine), (b) diglycidyl ether of bisphenol A (DGEBA), (c) 1,3-phenylenediamine (PDA), (d) 4,4′-methylenedianiline (MDA), and (e) 4,4′-diaminodiphenyl sulfone (DDS).

Sample Preparation. The protonated form of C18 amine was prepared by dissolving the amine in 100 mL of a 1 M HCl solution mixed with an equivalent amount of water and ethanol at 70 °C. Layered silicates were dispersed in the above solution and mixed vigorously for a day at 75 °C. C18 amine-treated clay (C18 clay) was washed with hot water and ethanol and filtered until no chlorine anion was detected in an $AgNO_3$ test. Then, it was dried in a vacuum for several days.

After epoxy resin was mixed with C18 clay for 1 h at 80 °C, an equivalent amount of aromatic diamine curing agent was dissolved in the mixture by heating to 120 °C. Homogeneous epoxy resin−aromatic diamine−clay mixtures were degassed in a vacuum oven at 70 °C, poured into a silicone mold, and then cured by two-step isothermal curing: 75 °C for 2 h and 150 °C for 2 h for DGEBA−PDA and DGEBA−MDA and 150 °C for 2 h and 175 °C for 2 h for DGEBA−DDS.

Characterization. X-ray diffraction patterns were obtained by using a homemade X-ray diffractometer (Hüls) with Ni-filtered Cu Ka radiation (λ = 0.1542 nm). Isothermal time-resolved X-ray diffraction studies were performed on the 3C2 (X-ray diffraction) and 4C1 (small-angle X-ray scattering) beamlines at the Pohang Accelerator Laboratory (PAL) to investigate the real time exfoliation behavior of clay layers in the epoxy−clay nanocomposites during the curing process. The primary beam was monochromized with two Si(111) single crystals at a wavelength of 0.1598 nm (the photon energy of the X-ray is 7.76 keV). Then, the X-ray beam was focused on a detector plane by a bent cylindrical mirror. The sample thickness was about 1 mm, the exposure time was 60 s, and the total data collection time was 90 min/sample. The detecting range was from 0.16 to 1.95 nm^{-1} in q value.

Transmission electron micrographs were obtained from the TEM JEOL 1200EX to investigate the morphology of epoxy−clay nanocomposites. The TEM samples were prepared by using the Ultramicrotome RMC MT7200 with a 45° diamond knife and mounted on 200-mesh copper grids.

The degree of conversion of epoxy−clay nanocomposites was measured in an isothermal curing experiment in a Perkin-Elmer DSC 7 at 120, 130, and 140 °C for 2 h and from dynamic scans in the range from 50 to 300 °C at a heating rate of 10 °C/min under a nitrogen atmosphere. The degree of conversion was defined as follows,

$$\alpha(t) = \frac{\int_0^t H(t)\,\mathrm{d}t}{\int_0^{120} H(t)\,\mathrm{d}t + H_{\mathrm{residual}}} = \frac{\int_0^t H(t)\,\mathrm{d}t}{H_{\mathrm{total}}}$$

(25) Vaia, R. A.; Jandt, K. D.; Kramer, E. J.; Giannelis, E. P. *Macromolecules* **1995**, *28*, 8080.
(26) (a) Vaia, R. A.; Giannelis, E. P. *Macromolecules* **1997**, *30*, 7990. (b) Vaia, R. A.; Giannelis, E. P. *Macromolecules* **1997**, *30*, 8000.
(27) Giannelis, E. P.; Krishnamoorti, R.; Manias, E. *Adv. Mater.* **1999**, *138*, 107.
(28) Balazs, A. C.; Singh, C.; Zhulina, E. *Macromolecules* **1998**, *31*, 8370.
(29) Lee, J. Y.; Baljon, A. R. C.; Loring, R. F.; Panagiotopoulos, A. Z. *J. Chem. Phys.* **1998**, *109*, 10321.
(30) Lee, J. Y.; Baljon, A. R. C.; Loring, R. F. *J. Chem. Phys.* **1999**, *111*, 9754.
(31) Manias, E.; Chen, H.; Krishnamoorti, R.; Genzer, J.; Kramer, E. J.; Giannelis, E. P. *Macromolecules* **2000**, *33*, 7955.
(32) Ginzburg, V. V.; Balazs, A. C. *Adv. Mater.* **2000**, *12*, 1805.

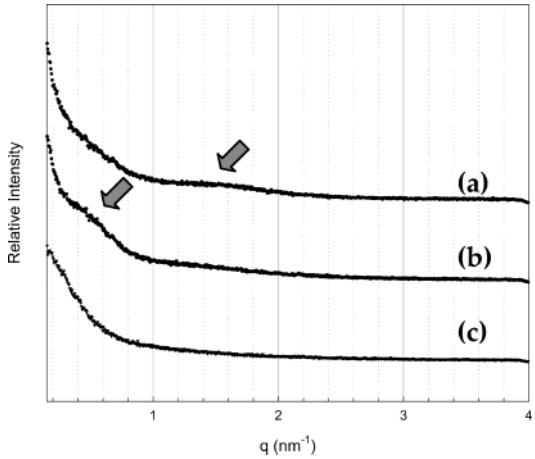

Figure 2. X-ray diffraction patterns for the epoxy-layered silicate nanocomposites with different curing agents: (a) DGEGBA−PDA−C18 clay (10 phr), (b) DGEBA−MDA−C18 clay (10 phr), and (c) DGEBA−DDS−C18 clay (10 phr).

where $\alpha(t)$ corresponds to the degree of conversion at time t (min), $H(t)$ to the heat of polymerization at time t, $H_{residual}$ to the residual heat of polymerization obtained from the dynamic scan after the isothermal scan, and H_{total} to the total heat of polymerization.

Results and Discussion

The XRD patterns in Figure 2 show the effects of electronegativity of amine curing agents on the exfoliation of the clay layer. DGEBA−DDS−C18 clay nanocomposites do not show any diffraction peak after curing, while diffraction peaks are observed at $q = 1.5$ and 0.6 for DGEBA−PDA−C18 clay and $q = 0.55$ for DGEBA−MDA−C18 clay nanocomposites. Clay layers can be exfoliated sufficiently in the epoxy with less reactive amine curing agent, that is, low electronegativity amine, such as DDS. Slow polymerization due to the low electronegativity of DDS ($pK_a = 2.15$)[33] in the DGEBA−DDS system provides low viscous medium to clay layer. Therefore, layered silicates can be exfoliated before the gelation of epoxy resin. However, epoxy−clay nanocomposites with PDA and MDA as curing agents have simply intercalated or partially exfoliated since PDA ($pK_a = 4.80$) and MDA (pK_a of MDA is located between that of PDA and DDS)[33] have electronegativity (reactivity) higher than DDS.

Figure 3 shows TEM morphologies of epoxy−clay nanocomposites with MDA and DDS as curing agents. In DGEBA−MDA−C18 clay nanocomposite (Figure 3a), the interlayer distance is about 10 nm or less and several clay layers are still agglomerated. On the other hand, DGEBA−DDS−C18 clay nanocomposite (Figure 3b) show that the interlayer distance of clay layer is more than 20 nm and that clay layers are separated layer by layer.

From the studies of XRD and TEM, it is observed that low reactivity of curing agent induces the exfoliated nanostructure since slow curing of epoxy resin delays the extragallery gelation and provides enough time for the intergallery polymerization.

To investigate the intercalation behavior of DGEBA in the intergallery of C18 clay, isothermal time-resolved

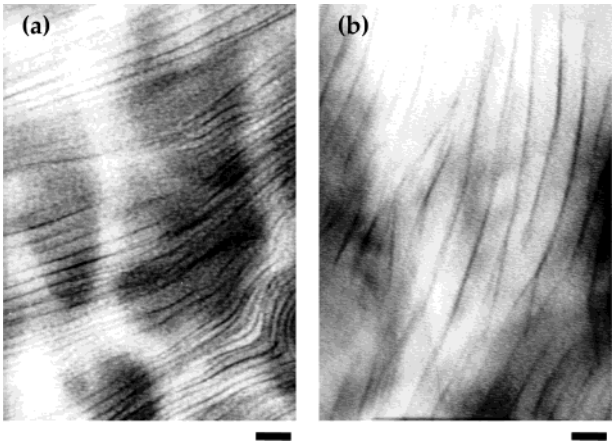

Figure 3. Transmission electron micrographs of (a) DGEBA−MDA−C18 clay (10 phr) and (b) DGEBA−DDS−C18 clay (10phr). Scale bar indicates 20 nm.

small-angle X-ray diffraction (SAXD) studies were conducted without curing agents by using small-angle X-ray diffraction beam lines in Pohang Accelerator Lab. Figure 4 shows the expanding behavior of C18 clay layers in a DGEBA−C18 clay mixture at room temperature and at 50 °C. A new diffraction peak at $q = 1.8$ was growing, and the diffraction peak at $q = 3.7$ was decreasing with time at 50 °C, while no change in the diffraction peak was observed at room temperature even after 1 h. Intercalant molecules, DGEBA, should have sufficient mobility as well as the miscibility with organic modifier, octadecylamine, to diffuse into the tiny gap (1.11 nm of intergallery height) of C18 clay. It appears that at 50 °C DGEBA has sufficient thermal energy and diffuses into the intergallery of C18 clay from the edge to the inner region. Considering that the basal spacing of the C18 clay layer did not increase gradually but jumped from $d_{001} = 1.77$ nm to $d_{001} = 3.49$ nm at 50 °C (Figure 4b), it appears that C18 amine attached on the edge part of the clay interacts with DGEBA molecules and changes configuration from mono- or bi-slanting form to bi-lipid form (perpendicular to the clay surface).[18] This fast reorientation of C18 amine molecule and elastic silicate layers induces a sudden increase of interlayer distance (Figure 5). Thus, DGEBA diffuses continuously into the inner region of the intergallery of C18 clay.

The intercalation and exfoliation behavior of epoxy−C18 clay nanocomposites during the curing process were investigated by varying the electronegativity of aromatic diamine curing agent and the curing temperature, using the same equipment in PAL as mentioned above. Figure 6 shows that the initial diffraction peak of DGEBA−PDA−C18 clay (5 phr) mixture decreases with time, but it does not disappear at both temperatures of 75 and 100 °C even after 30 min. And a new diffraction peak appears at $q = \sim 0.6$ after 20 min at 75 °C and 12 min at 100 °C.

Figure 7 shows the time-resolved SAXD patterns of DGEBA−DDS−C18 clay (5 phr) mixture cured at 120, 130, and 140 °C. The initial peak revealing the intercalation of DGEBA into the clay layers decreases with curing time, which is similar to the DGEBA−PDA−C18 clay mixture. As the initial diffraction peak was broadening until it disappeared finally in the DGEBA−DDS−C18 clay mixture, a new diffraction peak was generating

(33) Zubkov, V. A.; Koton, M. M.; Kudryavtsev, V. V.; Svetlichnyi, V. M. *Zh. Org. Khim.* **1981**, *17*, 1682.

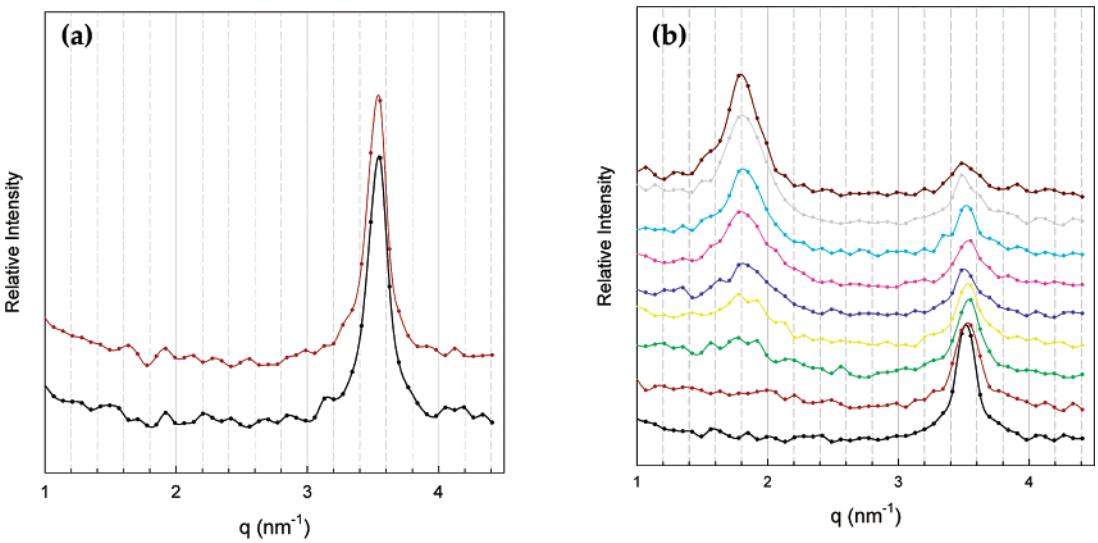

Figure 4. Isothermal time-resolved SXRD patterns of a DGEBA−C18 clay mixture at (a) room temperature and (b) 50 °C. These XRD patterns are displaced vertically for clarity, with scan time (min) from bottom to top as follows: 0 and 60 min in (a) and 0, 3, 6, 9, 12, 15, 22.5, 30, and 60 min in (b).

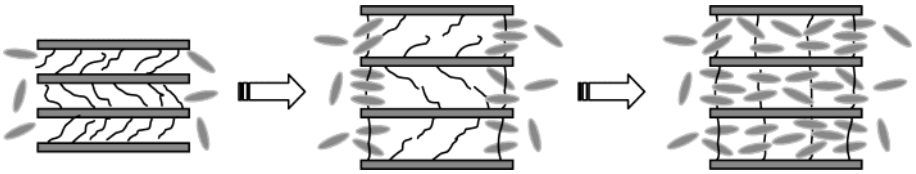

Figure 5. Schematic figures for the exfoliation process of clay layers with DGEBA on the mixing process.

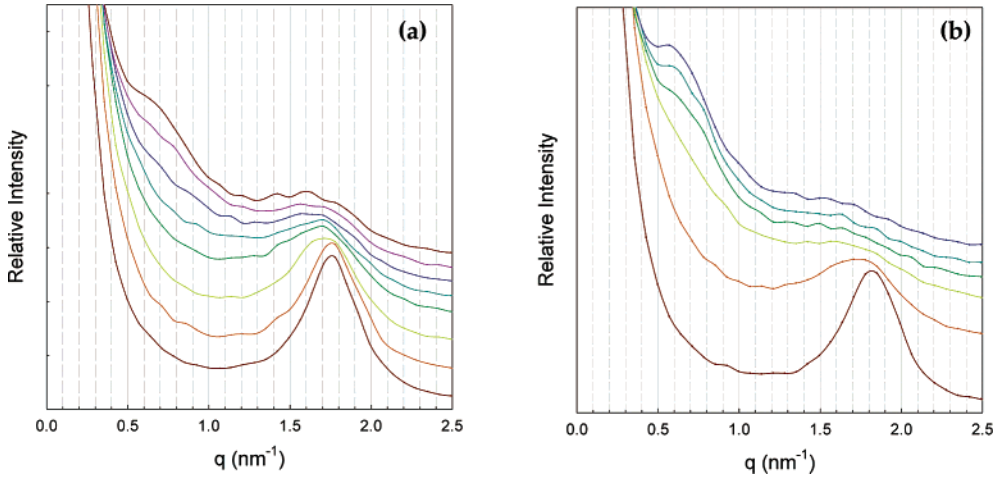

Figure 6. Isothermal time-resolved SXRD patterns of the DGEBA−PDA−C18 clay (5 phr) mixture at (a) 75 °C and (b) 100 °C. These XRD patterns are displaced vertically for clarity, with scan time (min) from bottom to top as follows: 0, 3, 6, 9, 12, 15, 21, and 30 min in (a) and 0, 3, 6, 9, 12, and 33 min in (b).

at $q = 0.6-0.7$ and shifting to the lower q value with the increase of curing time. This intercalated clay peak moved to the much lower q value and finally went over the undetectable region under the isothermal 140 °C curing condition. These results show a trend similar to that in the previous report.[18] It means that the balance of polymerization rate between the intergallery and extragallery region plays an important role in the exfoliation of clay layers with the epoxy matrix.

Figure 8 shows the summary of the exfoliation behavior of clay layer that depends on curing time and temperature in the DGEBA−DDS−C18 clay (5 phr) mixture. d1 and d2 in the legend indicate the peaks at small and large q values, respectively, and 120, 130, and 140 in the legend represent isothermal curing temperatures. After the interlayer distance increases suddenly at early time (about 18, 10, and 3 min at 120, 130, and 140 °C, respectively), a higher curing temperature introduces a faster increase of interlayer distance. The well-exfoliated structure (more than 20 nm of d spacing) of clay layers was obtained at a curing temperature higher than 130 °C in a DGEBA−DDS−C18 clay mixture, whereas the intercalated structure (<10 nm) was observed at both curing temperatures, 75 and 100 °C in the DGEBA−PDA−C18 clay mixture. This change was caused by fast network formation and matrix gelation (Figure 6). At lower than 120 °C of curing temperature in the DGEBA−DDS−C18 clay mixture, the fully exfoliated structure could not be observed within 90 min because the epoxy network has an extent

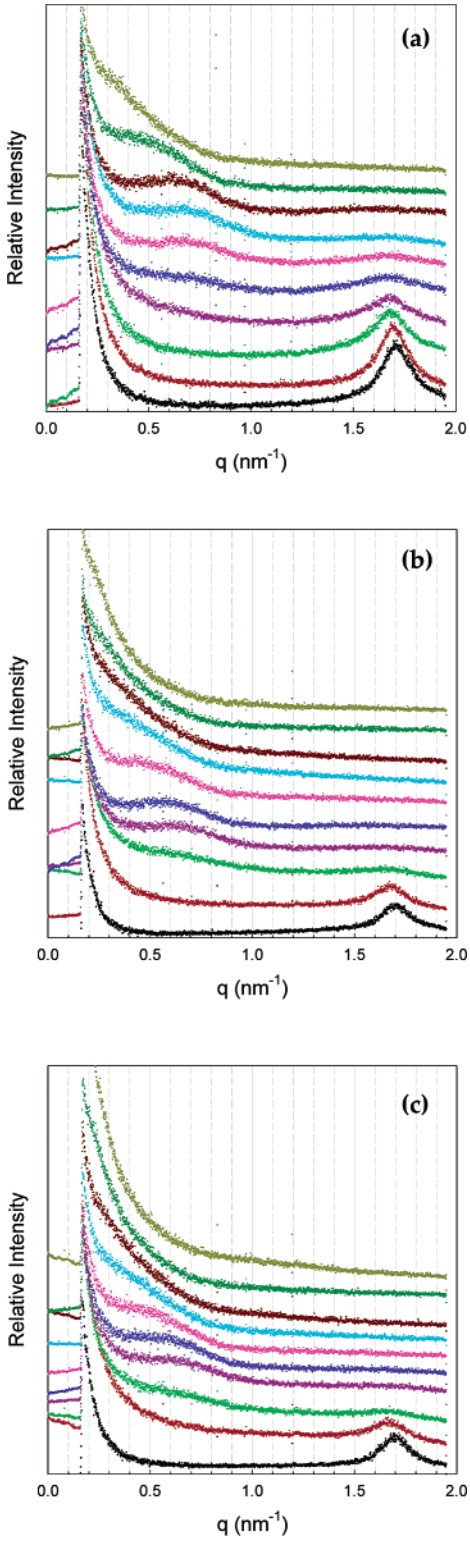

Figure 7. Isothermal time-resolved SXRD patterns of DGEBA−DDS−C18 clay (5 phr) at (a) 120 °C, (b) 130 °C, and (c) 140 °C. These XRD patterns are displaced vertically for clarity, with scan time (min) from bottom to top as follows: 0, 5, 11, 15, 20, 25, 30, 40, 60, and 89 min in (a), 0, 5, 10, 15, 20, 25, 30, 35, 40, and 76 min in (b) and 0, 3, 5, 7, 9, 11, 13, 15, 20, and 30 min in (c).

of conversion, which is too low to exfoliate the clay layers although a discrete increase (jumping phenomena) of the interlayer distance was also observed.

The exfoliation behavior of clay layers with increasing extent of epoxy conversion was demonstrated in Figure

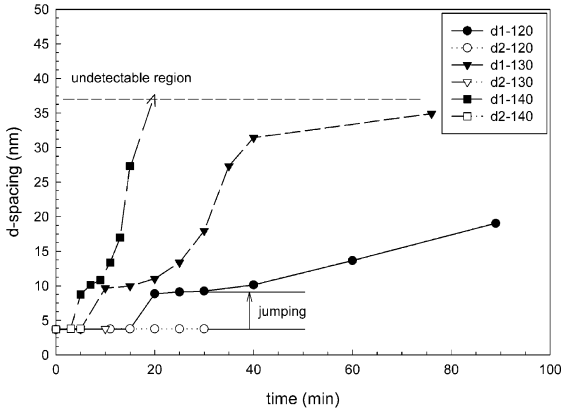

Figure 8. *d* spacing of clay layers with curing time at isothermal curing temperatures of 120, 130, and 140 °C in the DGEBA−DDS−C18 clay (5 phr).

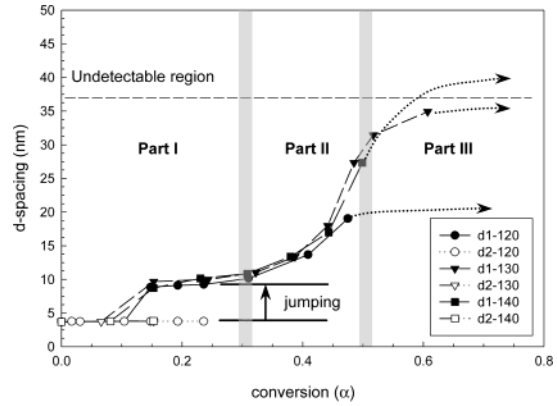

Figure 9. *d* spacing of clay layers with the degree of conversion at isothermal curing temperatures of 120, 130, and 140 °C in the DGEBA−DDS−C18 clay (5 phr). Dashed arrow lines indicate the expected trend of exfoliation behavior at each curing temperature.

Scheme 1[34]

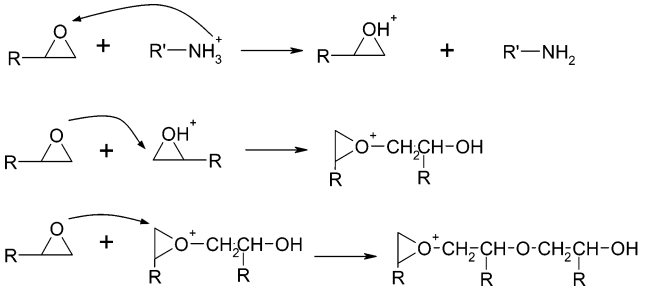

9. An expanded configuration (10 nm of interlayer distance) of clay layers was first observed after 15% of conversion, and it was maintained until 25−30% of conversion. Another discrete increase of interlayer distance occurred between 30 and 50% of conversion. The overall exfoliation behavior converges into an S-shape increase pattern with the extent of conversion at any curing temperature.

It was speculated that DGEBA might have been self-polymerized in directions parallel to the clay surface by the catalytic effect of protonated alkylammonium cation (Scheme 1[34]) at the first stage of isothermal curing reaction up to 15% of conversion.

(34) Lan, T.; Kaviratna, P. D.; Pinnavaia, T. J. *J. Phys. Chem. Soilds* **1996**, *57*, 1005.

Epoxy resin at the first stage it appears is a linear structure rather than a 3-D network structure since the self-polymerization of DGEBA by protonated C18 amine is faster than the curing reaction with aromatic diamines, and further extension of linear epoxy resin is restricted because of the confined geometry of intergallery region. A new peak at the small angle appears in XRD patterns (Figures 6 and 7), indicating a discrete increase of interlayer distance by the translation and expansion of clay layer in the inner region. And the initial peak broadens and decreases, which implies that the clay layer is folding from the outermost layer. From the TEM micrographs, clay layer folding was observed (Figure 3). The folding layer seems to come from the pressure applied to the clay layer as the polymerization reaction of epoxy resin proceeds in the intergallery region.

According to the coarse-grained simulation results of Bharadwaj et al.,[35] fully flexible clay layers show the total intercalation and relative translation with respect to each other in the polymer melt intercalation process. On the other hand, clay layers having an intermediate degree of flexibility are intercalated and folded in a sequential manner, starting with the outermost layer. Therefore, SWy-2 clay used in this study seems to have an intermediate degree of flexibility. However, the simulation result does not describe our system precisely. It shows just approximate physical properties of the clay layer. While the fixed values of molecular size and layer dimensions were used in simulation, our polymer molecules are changing in size with polymerization time and the real clay has many different physical properties and dimensions.

The unique S-shaped increase pattern of interlayer distance could be explained by the increase of extent of conversion in three different parts. In the first part between 0 and 30% of conversion, showing the increase of interlayer distance of <1 nm, epoxy resin was cured by the catalytic effect of protonated C18 cation to form linear polymers in the intergallery region rather than cross-linked networks. During this period, the expanded interlayer space was filled with epoxy resin growing in a direction parallel to the clay layer.

In the second part between 30 and 50% of conversion, the cross-linking reaction of DGEBA with DDS proceeded in the intergallery region since the protonated alkylammonium cation was already consumed. And the continued cross-linking reaction of epoxy resins increased the interlayer distance from 10 to 30 nm. At 130 and 140 °C of curing, the cross-linking from epoxy−amine reaction was enhanced by the catalytic effect of hydroxyl groups produced from self-polymerization and C18 amine.[36,37] However, at 120 °C of curing, the exfoliation of clay layer ended at 20 nm of interlayer distance because of the too slow cross-linking of DGEBA−DDS.

In the third part after 50% of conversion, the input rate of DGEBA into the intergallery decreased and more epoxy resin reacted in the extragallery region since the viscosity of DGEBA−DDS−C18 clay mixture increased. Therefore, the interlayer distance increased slowly and was then saturated.

Considering this exfoliation mechanism in relation to the reactivity of aromatic amine curing agents, DGEBA−C18 clay cured with more reactive PDA was always showing two states for the total curing process (Figure 2a and Figure 6); the intercalation state of DGEBA and the first jumping state due to self-polymerized epoxy (part I in Figure 9). Although the initial Bragg reflection peak at $q = 1.75-1.8$ changed slightly to the low angle and a new peak was generating at $q = 0.6$, all clay layers did not move to a new expanded state. It means that immature self-polymerized epoxy polymer in the intergallery region could not gain enough volume and time to push away all the clay layers before the matrix gelation. In Figure 2b, DGEBA−C18 clay cured with MDA of intermediate reactivity in this study did not show the initial reflection peak unlike the DGEBA−PDA−C18 clay system. However, the nanostructure of DGEBA−MDA−C18 clay did not proceed to the further exfoliation step (part II or part III) but was fixed in the part I state because the growth rate of polymer in the intergallery region was too slow to come up with an increasing rate of the extragallery viscosity.

Conclusions

Nanostructures in epoxy−clay nanocomposites were controlled by changing chemical and thermal curing conditions in the intergallery region. In this study, the exfoliated nanostructure was achieved either by retarding the cross-linking reaction in the extragallery region with a low reactive aromatic diamine curing agent or by an increase in the curing temperature.

It is interesting to note that the clay layers are exfoliated stepwise rather than gradually. Three steep increases of the interlayer distance were observed in the total epoxy−clay nanocomposite manufacturing process. The first increase comes from the intercalation of DGEBA into the intergallery region of C18 clay. The second increase is caused by the clay layer folding, translating and expanding from the self-polymerization of DGEBA with the catalytic effect of protonated C18 amine cation. The third increase takes place from the cross-linking of epoxy resin with C18 amine and the amine curing agent in the intergallery region. It is important to enhance the cross-linking in the intergallery region for the well-exfoliated nanostructure.

As internal epoxy monomer is polymerizing and filling the free space in the intergallery region, the pressure is building on the clay layer without a significant change in nanostructure. When the pressure applied on the clay layer exceeds a critical point to keep the current nanostructure, the intergallery region may be enlarged suddenly.

Acknowledgment. This work was supported by the Korea Ministry of Commerce, Industry and Energy ("Next Generation New Technology Development of High Performance Nanocomposites" project), and it was partially supported also by the Korea Ministry of Science and Technology (National Research Laboratories Program).

CM0205837

(35) Bharadwaj, R. K.; Vaia, R. A.; Farmer, B. L. In *Polymer Nanocomposites−Synthesis, Characterization, and Modeling*; Krishnamoorti, R., Vaia, R. A., Eds.; ACS Symposium Series; American Chemical Society: Washington, DC, 2002.

(36) *Epoxy Resins*, 2nd ed.; May, C. A., Ed.; Marcel Dekker: New York, 1988.

(37) *Chemistry and Technology of Epoxy Resins*; Ellis, B., Ed.; Blackie Academic & Professional: London, 1993.